WOODHEAD PUBLISHING SERIES IN CIVIL AND STRUCTURAL ENGINEERING

# SEISMIC EVALUATION, DAMAGE, AND MITIGATION IN STRUCTURES

Edited by
IMAN MANSOURI
PAUL O. AWOYERA

ELSEVIER

# Contents

# Controlling the deflection of long steel beams using pretensioned cables

2

*Nader Fanaie*[1] *and Fatemeh Partovi*[2]
[1]Department of Civil Engineering, K. N. Toosi University of Technology, Tehran, Iran,
[2]School of Engineering, University of British Columbia, Kelowna, BC, Canada

## Notations

| | |
|---|---|
| $\Delta \mathbf{F}$ | the increment of the pretensioning force in the cable |
| $\boldsymbol{M(x)}$ | bending moment |
| $\boldsymbol{U}$ | total strain energy |
| $\boldsymbol{q}$ | uniform distributed load |
| $\boldsymbol{l_b}$ | beam length |
| $\boldsymbol{l_c}$ | inclined cable length |
| $\boldsymbol{A_b}$ | cross-sectional area of beam |
| $\boldsymbol{A_c}$ | cross-sectional area of cable on both sides of the web |
| $\boldsymbol{E_b}$ | elasticity modulus of beam |
| $\boldsymbol{E_c}$ | elasticity modulus of cable |
| $\boldsymbol{I_b}$ | moment of inertia of beam |
| $\boldsymbol{\theta}$ | angle of inclined cable with the horizontal axis |
| $\boldsymbol{y_0}$ | distance of neutral axis to the connection point of steel cable to the beam flange (half of the height of beam web) |
| $\boldsymbol{a}$ | the distance between the inclination change region of the cable and the support (horizontal projection of inclined cable) |
| $\boldsymbol{l_{c1}}$ | the lengths of the first inclined cables, $c1$ |
| $\boldsymbol{l_{c2}}$ | the lengths of the second inclined cables, $c2$ |
| $\boldsymbol{\theta_1}$ | the angle between the first inclined cable and horizontal axis |
| $\boldsymbol{\theta_2}$ | the angle between the second inclined cable and horizontal axis |
| $\boldsymbol{M}$ | fixed end moment |
| $\boldsymbol{F}$ | total cable force |
| $\boldsymbol{F_{pt}}$ | initial pretensioning force of the cable |
| $\Delta$ | maximum deflection |
| $\boldsymbol{m(x)}$ | bending moment under virtual loading |

## 2.1 Introduction

Cables as essential structural elements can withstand tensile force and, in general, improve the bearing capacity and the structure's stiffness [1]. Structural applications of steel cables have been recently increased in the construction industry. Hou

**Seismic Evaluation, Damage, and Mitigation in Structures. DOI: https://doi.org/10.1016/B978-0-323-88530-0.00003-9**

and Tagawa [2] established an innovative seismic rehabilitation method to promote steel flexural frames using cable-cylinder bracing. It was reported that this method improves the story's lateral strength without reducing the flexural frame's ductility. Fanaie et al. [3] proposed theoretical equations for the system of cable-cylinder bracing employing a rigid cylinder such as a steel cylinder. They validated the results using Abaqus [4] finite element (FE) models. The authors further investigated seismic performance of steel flexural frames reinforced by cable-cylinder bracing and achieved acceptable conclusions [5]. Giaccu [6] studied the nonlinear dynamic response of pretensioned-cable cross-braced structures while there was slackening in the braces. He found a direct correlation between equivalent frequency and slackening in the braces.

The most effective way to reduce the steel requirements and to improve the bearing capacity of steel beams is to pretension them using high-strength cables. The first and foremost structure that was pretensioned was the reinforced concrete structure. Brunesi et al. [7] investigated numerically and experimentally the shear capacity of precast-prestressed hollow-core slabs. Based on the obtained results, they showed that peak shear stress was localized at the bottom side of the cross section rather than at the level of the centroid. Al-Negheimish et al. [8] experimentally studied the long-term deflection of prestressed hollow core slabs. They compared their results with the predictions of the effective modulus approach, which considers the creep and shrinkage models recommended by ACI 209 Committee [9]. The pretensioned steel cables in steel beams were used by Dischinger and Magnel for the first time. The pretensioned steel structures are being built around the world, particularly in the United States, Germany, and Russia. This illustrates the economic and structural advantages of pretensioned steel beams comparing with the nonprestressed beams. The method of pretensioning is proper for constructing new structures and reinforcing the existing ones [10].

Many studies have been conducted to evaluate the performance of pretensioned concrete and composite beams applying steel cables. Le et al. [11] experimentally investigated the use of both unbonded carbon fiber−reinforced polymer (CFRP) tendons and steel tendons on precast T-section segmental concrete. They demonstrated that CFRP tendons could replace steel tendons, and the beams attained both good strength and ductility capacity. Pisani [12] analyzed the simply supported concrete beam externally prestressed under sustained loads. He developed two numerical methods capable of representing the time evolution of both the stress distribution and the displacements of a simply supported concrete beam prestressed externally. He also provided an instance to calibrate the accuracy of the methods. Lou et al. [13] numerically investigated the flexural response of continuous externally fiber-reinforced polymer prestressed concrete beams including different linearly transformed cable profiles. According to the results, they concluded that the cable shift by linear transformation does not affect the basic performance at all stages of loading up to failure. They also confirmed that the secondary moments differ linearly with the cable shift. Ayyub et al. [14,15] experimentally and analytically evaluated prestressed steel-concrete composite beams benefiting steel cable, wherever there are positive or negative bending moments. It was revealed that

pretensioning increased the ultimate strength. Nie et al. [16] derived theoretical equations to obtain both yield and deflection and ultimate moments of prestressed steel-concrete composite beam, which was simply supported regarding the effect of slip. They compared the experimental results to the suggested formulas. Zhou et al. [17] performed the empirical investigation and numerical modeling of prestressed composite beams exposed to positive moment and fire. They showed that the cable strands' stress highly affected the fire resistance of composite beams, which were prestressed with external tendons. Some scholars have explored the behavior of prestressed steel beams with steel cables, including Troitsky [10] who examined that utilizing cables. He concluded that steel cables increase the stiffness of the beam and reduces its deformation. Belletti and Gasperi [18] analyzed the performance of I-shaped steel beams, which were simply supported and prestressed by tendons, emphasizing two parameters, including the value of prestressing force and the number of deviators. The flexural behavior of steel I-beam prestressed with externally unbonded tendons was analytically and experimentally investigated by Park et al. [19]. It was deduced that the yielding and ultimate bearing capacity of steel I-beam were significantly increased. Fanaie et al. [20–22] utilized the methods of least work and virtual work to generate theoretical relations for calculating the increment in the pretensioning force of cables due to the external loading and the steel beams' deflection having various support conditions and cable patterns, respectively. To validate the theoretical relations, they developed numerical models of steel beams with different support conditions and cable patterns in the Abaqus FE software. Kambal and Jia [23] proposed an FE model to examine the effectiveness of the prestressing method regarding the flexural behavior of a steel box girder, which was simply supported. They confirmed the preciseness of the suggested formulation with the experimental results. Zhang [24] investigated the analytical solutions for the symmetric and antisymmetric elastic lateral-torsional buckling of prestressed I-shaped steel beams with equal end moments and rectilinear tendons. Thai et al. [25] analyzed various types of cable net and optimized their volume as an objective function. They considered the allowable stress and maximum displacement as the optimization restrictions. They applied the appropriate pretensioning forces to the cable nets to decrease the displacement of the structure and achieved an optimum volume. According to the results, they indicated that when the displacement constraint was relatively small or the allowable stress was relatively large, the pretensioning forces performed a critical role in achieving the optimum volume.

Controlling the deflection of beams (specifically long beams) causes challenges for the structural designers. Therefore this research focused on controlling the deflection of steel beams with different support conditions and cable patterns. The increment in the pretensioning force of the cable under external loading can be obtained based on the least work method. The relations of maximum deflection of steel beams with various cable patterns are derived then benefiting the virtual work method. Eventually, the theoretical relations are verified with numerical models.

## 2.2 The pretensioned symmetric I-shaped steel beams with steel cables

As shown in Fig. 2.1, symmetric I-shaped steel beams, which have different support conditions, that is, simply supported, fixed supported, and cantilever beams, are pretensioned with varying cable patterns employed in both sides of the web and under external loading. It is observed that the cables are restrained to the top flange of the beam at both ends. After that, they pass through the deviators on the bottom flange of the beam and produce a V-shaped pattern, a modified V-shaped pattern and accompanied by two V-shaped patterns [20−22].

The following hypotheses are considered to analyze the pretensioned symmetric steel I-beams with steel cables:

1. The cable and steel beam are made of a linearly elastic material.
2. The deformations are small.
3. The shear deformation is not included.
4. The friction loss and the relaxation of a steel cable are not taken into account.
5. The steel section is compact and hot rolled.

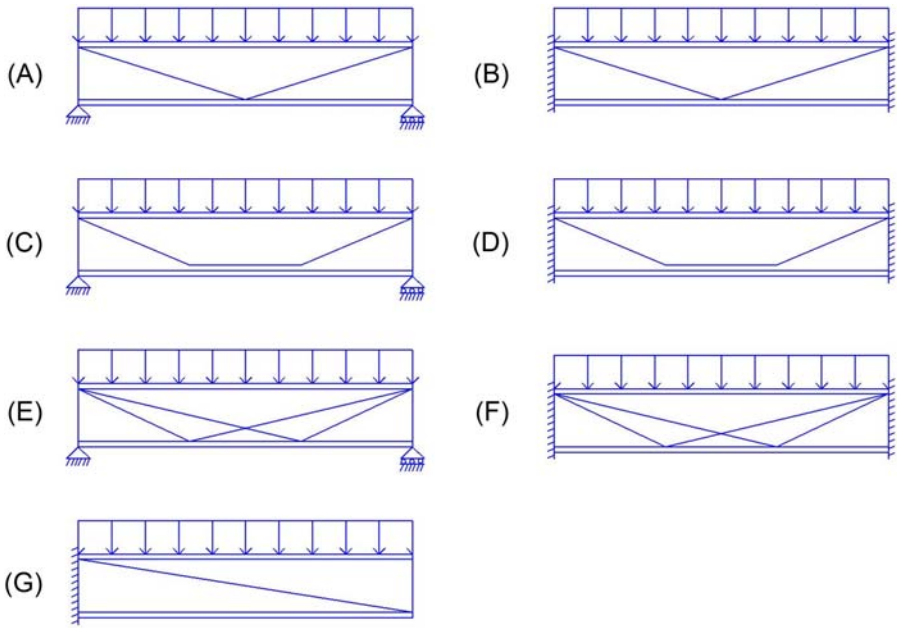


**Figure 2.1** Pretensioned symmetric steel I-beams with steel cables subjected to external loading: (A) a beam with simple supports and the V-shaped cable pattern; (B) a beam with fixed supports and the V-shaped cable pattern; (C) a beam with simple supports and the modified V-shaped cable pattern; (D) a beam with fixed supports and the modified V-shaped cable pattern; (E) a beam with simple supports and two V-shaped cable patterns; (F) a beam with fixed supports and two V-shaped cable patterns; (G) a cantilever beam with steel cables.

## 2.3 The increment of the pretensioning force in the cable under external loading

The distributed loading is uniform, therefore the length of the cable increases by $\Delta L$, causing the pretensioning force in the cable, $F_{pt}$, to increase by $\Delta F$. The structure is statically indeterminate and the static equilibrium relations are not enough to determine $\Delta F$. As a result, the least work method can be used to determine the pretensioning force's increment in the cable.

Based on the least work method, the relation of the steel beam's total strain energy caused by the axial force and the bending moment is differentiated to $\Delta F$. Also, the total strain energy of the cable due to its axial force is differentiated to $\Delta F$. The increment of the pretensioning force in the cable, $\Delta F$, was calculated by equating the result to zero.

### 2.3.1 The beam with simple supports and the V-shaped cable pattern

The increment of the pretensioning force in the cable equals $\Delta F$ in the beam with simple supports and the V-shaped cable pattern (Fig. 2.2). Accordingly, the axial force of the beam equals $\Delta F\cos\theta$. Furthermore, the bending moment and eventually the resulting strain energy can be calculated for half of the beam in a symmetric structure with a symmetric loading (Fig. 2.2). The strain energy is duplicated then to obtain the bending strain energy of the beam in whole. Therefore the bending moment for half of the beam with simple supports and the V-shaped cable pattern subjected to uniform distributed loading is determined using the following relation [20]:

For $0 \leq x \leq \frac{l_b}{2}$ range:

$$M(x) = \Delta F cos\theta y_0 - \left(\Delta F sin\theta - \frac{ql_b}{2}\right)x - \frac{qx^2}{2} \tag{2.1}$$

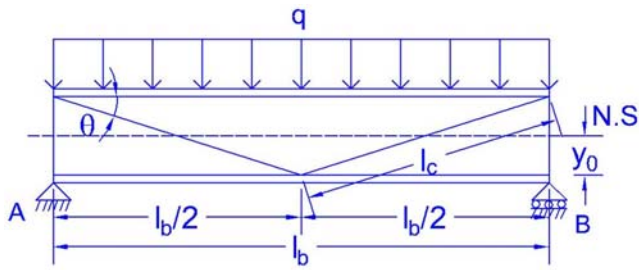


**Figure 2.2** The beam with simple supports and the V-shaped cable pattern.

Because both the structure and the loading are symmetric, the equation of total strain energy is obtained as below:

$$U = 2 \times \frac{1}{2(EI)_b} \int_0^{\frac{l_b}{2}} \left( \Delta F cos\theta y_0 - \left( \Delta F sin\theta - \frac{ql_b}{2} \right) x - \frac{qx^2}{2} \right)^2 dx + 2 \times \frac{\Delta F^2 l_c}{2(AE)_c} + \frac{(\Delta F cos\theta)^2 l_b}{2(AE)_b}$$

$$= \frac{1}{(EI)_b} \left\{ \begin{array}{c} \frac{q^2 l_b^5}{240} + \frac{\Delta F^2 l_b^3 sin^2\theta}{24} + \frac{\Delta F^2 l_b y_0^2 cos^2\theta}{2} \\ -\frac{\Delta F^2 l_b^2 y_0 sin\theta cos\theta}{4} - \frac{5q\Delta F l_b^4 sin\theta}{192} + \frac{q\Delta F l_b^3 y_0 cos\theta}{12} \end{array} \right\} + \frac{\Delta F^2 l_c}{(AE)_c} + \frac{\Delta F^2 l_b cos^2\theta}{2(AE)_b} \tag{2.2}$$

Using the least work method, differentiating the total strain energy equation to $\Delta F$, and equating the result to zero, the increase in the pretensioning force of the cable ($\Delta F$) is determined as below [20]:

$$\frac{\partial U}{\partial(\Delta F)} = 0 \tag{2.3}$$

$$\Delta F = \frac{5ql_b^4 sin\theta - 16ql_b^3 y_0 cos\theta}{16\left( l_b^3 sin^2\theta + 12l_b y_0^2 cos^2\theta - 6l_b^2 y_0 sin\theta cos\theta + \frac{24(EI)_b l_c}{(AE)_c} + \frac{12I_b l_b cos^2\theta}{A_b} \right)} \tag{2.4}$$

where $q$ presents uniform distributed load; $l_b$ and $l_c$ are used for the lengths of the beam and inclined cable, respectively; $A_b$ presents the cross section of the beam and $A_c$ presents the cross section of the cable at both sides of the web; $E_b$ and $E_c$ are used for modulus of the beam and cable, respectively; $I_b$ presents the steel section's moment of inertia; $y_0$ is used for the distance between the steel cable's connection point to the beam flanges (half of the height of the beam web) and the neutral surface; and finally, $\theta$ is the angle between the inclined cable and the horizontal axis.

### 2.3.2 The beam with simple supports and the modified V-shaped cable pattern

As it is presented in Fig. 2.3, in the beam with simple supports and the modified V-shaped cable pattern, the increment of the cable's pretensioning force equals $\Delta F$ in the inclined parts. It also equals $\Delta F \cos\theta$ in the horizontal part to maintain a constant bending moment within the region that cable inclination changes. Accordingly, the beam's

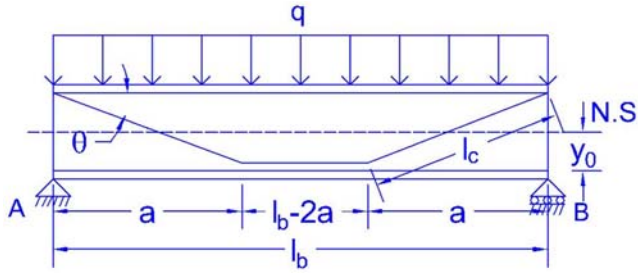


**Figure 2.3** The beam with simple supports and the modified V-shaped cable pattern.

axial force equals $\Delta F\cos\theta$. Therefore, as mentioned before, due to the existed symmetry in the structure and loading (Fig. 2.3), the bending moment for half of the beam with simple supports and the modified V-shaped cable pattern subjected to the uniform distributed loading is calculated by using the following relations [20]:

For $0 \leq x \leq a$ range,

$$M_1(x) = \Delta F cos\theta y_0 - \left(\Delta F sin\theta - \frac{ql_b}{2}\right)x - \frac{qx^2}{2} \tag{2.5}$$

For $a \leq x \leq \frac{l_b}{2}$ range,

$$M_2(x) = -\Delta F cos\theta y_0 + \frac{ql_b x}{2} - \frac{qx^2}{2} \tag{2.6}$$

Considering the existed symmetry in the structure and loading, the total strain energy equation can be obtained as below:

$$\begin{aligned} U &= 2 \times \frac{1}{2(EI)_b} \left\{ \begin{array}{c} \int_0^a \left(\Delta F cos\theta y_0 - \left(\Delta F sin\theta - \frac{ql_b}{2}\right)x - \frac{qx^2}{2}\right)^2 dx \\ + \int_a^{\frac{l_b}{2}} \left(-\Delta F cos\theta y_0 + \frac{ql_b x}{2} - \frac{qx^2}{2}\right)^2 dx \end{array} \right\} \\ &+ 2 \times \frac{\Delta F^2 l_c}{2(AE)_c} + \frac{(\Delta F cos\theta)^2 (l_b - 2a)}{2(AE)_c} + \frac{(\Delta F cos\theta)^2 l_b}{2(AE)_b} \\ &= \frac{1}{(EI)_b} \left\{ \begin{array}{c} \frac{q^2 l_b^5}{240} + \frac{\Delta F^2 a^3 sin^2\theta}{3} + \frac{\Delta F^2 l_b y_0^2 cos^2\theta}{2} - \Delta F^2 y_0 a^2 sin\theta cos\theta + \frac{q\Delta F a^4 sin\theta}{4} \\ - \frac{q\Delta F l_b a^3 sin\theta}{3} - \frac{2q\Delta F y_0 a^3 cos\theta}{3} + q\Delta F l_b y_0 a^2 cos\theta - \frac{q\Delta F l_b^3 y_0 cos\theta}{12} \end{array} \right\} \\ &+ \frac{\Delta F^2 l_c}{(AE)_c} + \frac{\Delta F^2 (l_b - 2a) cos^2\theta}{2(AE)_c} + \frac{\Delta F^2 l_b cos^2\theta}{2(AE)_b} \end{aligned} \tag{2.7}$$

Using the least work method, the increment of the cable's pretensioning force ($\Delta F$) is estimated by the following equation [20]:

$$\Delta F = \frac{-3qa^4 sin\theta + 4ql_b a^3 sin\theta + 8qy_0 a^3 cos\theta - 12ql_b y_0 a^2 cos\theta + ql_b^3 y_0 cos\theta}{4\left(2a^3 sin^2\theta + 3l_b y_0^2 cos^2\theta - 6y_0 a^2 sin\theta cos\theta + \frac{3(EI)_b}{(AE)_c}[2l_c + (l_b - 2a)cos^2\theta] + \frac{3l_b l_b cos^2\theta}{A_b}\right)} \tag{2.8}$$

where $a$ is the distance between the inclination change region of the cable and the support (horizontal projection of inclined cable).

In Eq. (2.8), when the length of the horizontal cable ($l_b - 2a$, as observed in Fig. 2.3) approaches zero, Eq. (2.4) is acquired related to the V-shaped cable pattern.

### 2.3.3 The beam with simple supports and two V-shaped cable patterns

In the beam with simple supports and two V-shaped cable patterns (Fig. 2.4), the increment of the pretensioning force in the cable equals $\Delta F$ in the first inclined part ($C_1$). It equals $\frac{\Delta F cos\theta_1}{cos\theta_2}$ in the second inclined part ($C_2$) to maintain a constant bending moment within the cable inclination change region. Accordingly, The axial force of the beam equals $2\Delta F cos\theta_1$. Therefore, as mentioned before, because the structure and the loading both are symmetric (Fig. 2.4), for half of the beam with simple supports and two V-shaped cable patterns subjected to the uniform distributed loading, the bending moment is calculated as below [21]:

For $0 \le x \le a$ range,

$$M_1(x) = 2\Delta F cos\theta_1 y_0 - \left(\Delta F sin\theta_1 + \Delta F cos\theta_1 tan\theta_2 - \frac{ql_b}{2}\right)x - \frac{qx^2}{2} \tag{2.9}$$

For $a \le x \le \frac{l_b}{2}$ range,

$$M_2(x) = -\Delta F cos\theta_1 tan\theta_2 a + \frac{ql_b x}{2} - \frac{qx^2}{2} \tag{2.10}$$

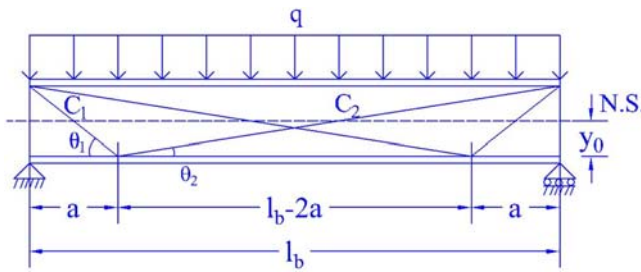


**Figure 2.4** The beam with simple supports and two V-shaped cable patterns.

Because the structure and the loading both are symmetric, the equation of total strain energy is obtained as below:

$$
\begin{aligned}
U = 2\times\frac{1}{2(EI)_b}&\left\{\begin{array}{c}\int_0^a\left(2\Delta F cos\theta_1 y_0-\left(\Delta F sin\theta_1+\Delta F cos\theta_1 tan\theta_2-\frac{ql_b}{2}\right)x-\frac{qx^2}{2}\right)^2dx\\ +\int_a^{\frac{l_b}{2}}\left(-\Delta F cos\theta_1 tan\theta_2 a+\frac{ql_bx}{2}-\frac{qx^2}{2}\right)^2dx\end{array}\right\}\\
&+2\times\frac{\Delta F^2 l_{c1}}{2(AE)_c}+2\times\frac{\left(\frac{\Delta F cos\theta_1}{cos\theta_2}\right)^2 l_{c2}}{2(AE)_c}+\frac{(2\Delta F cos\theta_1)^2 l_b}{2(AE)_b}\\
=\frac{1}{(EI)_b}&\left\{\begin{array}{c}4\Delta F^2 y_0^2 acos^2\theta_1+\frac{q^2l_b^5}{240}+\frac{q\Delta Fl_ba^3cos\theta_1tan\theta_2}{6}+q\Delta Fl_by_0a^2cos\theta_1\\ -\frac{q\Delta Fl_b^3acos\theta_1tan\theta_2}{12}-\frac{2\Delta F^2a^3cos^2\theta_1tan^2\theta_2}{3}+\frac{q\Delta Fa^4sin\theta_1}{4}\\ -\frac{q\Delta Fa^4cos\theta_1tan\theta_2}{12}-\frac{2q\Delta Fy_0a^3cos\theta_1}{3}+\frac{2\Delta F^2a^3sin\theta_1cos\theta_1tan\theta_2}{3}\\ -\frac{q\Delta Fl_ba^3sin\theta_1}{3}-2\Delta F^2y_0a^2sin\theta_1cos\theta_1-2\Delta F^2y_0a^2cos^2\theta_1tan\theta_2\\ +\frac{\Delta F^2l_ba^2cos^2\theta_1tan^2\theta_2}{2}+\frac{\Delta F^2a^3sin^2\theta_1}{3}\end{array}\right\}\\
&+\frac{\Delta F^2l_{c1}}{(AE)_c}+\frac{\Delta F^2l_{c2}cos^2\theta_1}{(AE)_ccos^2\theta_2}+\frac{2\Delta F^2l_bcos^2\theta_1}{(AE)_b}
\end{aligned}
\tag{2.11}
$$

Using the least work method, the pretensioning force's increment of the cable ($\Delta$F) is determined as below [21]:

$$
\Delta F=\frac{\begin{array}{c}-2ql_ba^3cos\theta_1tan\theta_2-12ql_by_0a^2cos\theta_1+ql_b^3acos\theta_1tan\theta_2\\ -3qa^4sin\theta_1+qa^4cos\theta_1tan\theta_2+8qy_0a^3cos\theta_1+4ql_ba^3sin\theta_1\end{array}}{4\left(\begin{array}{c}24y_0^2acos^2\theta_1-4a^3cos^2\theta_1tan^2\theta_2+4a^3sin\theta_1cos\theta_1tan\theta_2-12y_0a^2sin\theta_1cos\theta_1\\ -12y_0a^2cos^2\theta_1tan\theta_2+3l_ba^2cos^2\theta_1tan^2\theta_2+2a^3sin^2\theta_1\\ +\frac{6(EI)_b}{(AE)_c}\left[l_{c1}+\frac{l_{c2}cos^2\theta_1}{cos^2\theta_2}\right]+\frac{12I_bl_bcos^2\theta_1}{A_b}\end{array}\right)}
\tag{2.12}
$$

where $l_{c1}$ and $l_{c2}$ present the lengths of the first and the second inclined cables, $c1$ and $c2$, respectively. Meanwhile, $\theta_1$ presents the angle between the first inclined cable and horizontal axis, and $\theta_2$ is used for the angle between the second inclined cable and horizontal axis.

### 2.3.4 The beam with fixed supports and the V-shaped cable pattern

The increment of the cable's pretensioning force equals $\Delta F$ in the fixed supported beam along with the V-shaped cable pattern (Fig. 2.5). Consequently, the axial force of the beam equals $\Delta F\cos\theta$. Moreover, using the least work method, since there are two degrees of indeterminacy (the increment of the cable's pretensioning force, $\Delta F$, and the fixed end moment, $M$) in the beam with fixed supports and V-shaped cable pattern, the total strain energy equation should be differentiated to both $\Delta F$ and $M$ and then equals zero to obtain $\Delta F$ and $M$. Therefore the bending moment for half of the beam with fixed supports and the V-shaped cable pattern subjected to uniform distributed loading can be obtained by the following relation [20] in order to determine the total strain energy:

For $0 \le x \le \frac{l_b}{2}$ range,

$$M(x) = -M + \Delta F cos\theta y_0 - \left(\Delta F sin\theta - \frac{ql_b}{2}\right)x - \frac{qx^2}{2} \tag{2.13}$$

Because the structure and the loading both are symmetric, the relation of total strain energy is obtained as below:

$$U = 2 \times \frac{1}{2(EI)_b}\int_0^{\frac{l_b}{2}} \left(-M + \Delta F cos\theta y_0 - (\Delta F sin\theta - \tfrac{ql_b}{2})x - \tfrac{qx^2}{2}\right)^2 dx + 2 \times \frac{\Delta F^2 l_c}{2(AE)_c}$$
$$+ \frac{(\Delta F cos\theta)^2 l_b}{2(AE)_b} = \frac{1}{(EI)_b}\left\{\begin{array}{c} \frac{q^2 l_b^5}{240} + \frac{\Delta F^2 l_b^3 sin^2\theta}{24} + \frac{\Delta F^2 l_b y_0^2 cos^2\theta}{2} \\ -\frac{\Delta F^2 l_b^2 y_0 sin\theta cos\theta}{4} - \frac{5q\Delta F l_b^4 sin\theta}{192} + \frac{q\Delta F l_b^3 y_0 cos\theta}{12} \\ + \frac{M\Delta F l_b^2 sin\theta}{4} - M\Delta F l_b y_0 cos\theta - \frac{qMl_b^3}{12} + \frac{M^2 l_b}{2} \end{array}\right\}$$
$$+ \frac{\Delta F^2 l_c}{(AE)_c} + \frac{\Delta F^2 l_b cos^2\theta}{2(AE)_b} \tag{2.14}$$

Using the least work method, the fixed end moment ($M$) and the pretensioning force's increment of the cable ($\Delta F$) are calculated using the following equations [20]:

$$M = \frac{ql_b^2}{12} - \frac{\Delta F l_b sin\theta}{4} + \Delta F y_0 cos\theta \tag{2.15}$$

$$\Delta F = \frac{ql_b^4 sin\theta}{4\left(l_b^3 sin^2\theta + \frac{96(EI)_b l_c}{(AE)_c} + \frac{48 I_b l_b cos^2\theta}{A_b}\right)} \tag{2.16}$$

As Fig. 2.5 presents, if $sin\theta = \frac{2y_0}{l_c}$ and $cos\theta = \frac{l_b}{2l_c}$ were replaced in Eq. (2.16), the fixed end moment ($M$) would be equal to $\frac{ql_b^2}{12}$ related to the moment at a fixed end in steel beam without cable.

### 2.3.5 The beam with fixed supports and the modified V-shaped cable pattern

In the beam with fixed supports and the modified V-shaped cable pattern (Fig. 2.6), $\Delta F$ presents the increase in the cable's pretensioning force in the inclined parts. Pretensioning force of the cable in the horizontal part should be $\Delta F\cos\theta$ to maintain a constant bending moment at the cable inclination change region. Therefore the beam's axial force equals $\Delta F\cos\theta$. Moreover, the beam with fixed supports and the modified V-shaped cable pattern has two degrees of indeterminacy (the pretensioning force's increment of the cable, $\Delta F$, and the fixed end moment, $M$). Thus the bending moment for half of the beam with fixed supports and the modified V-shaped cable pattern subjected to uniform distributed loading is determined by the following relations [20] to obtain the total strain energy.

For $0 \leq x \leq a$ range,

$$M_1(x) = -M + \Delta F cos\theta y_0 - \left(\Delta F sin\theta - \frac{ql_b}{2}\right)x - \frac{qx^2}{2} \tag{2.17}$$

For $a \leq x \leq \frac{l_b}{2}$ range,

$$M_2(x) = -M - \Delta F cos\theta y_0 + \frac{ql_b x}{2} - \frac{qx^2}{2} \tag{2.18}$$

Because the structure and the loading both are symmetric, the total strain energy can be obtained as below:

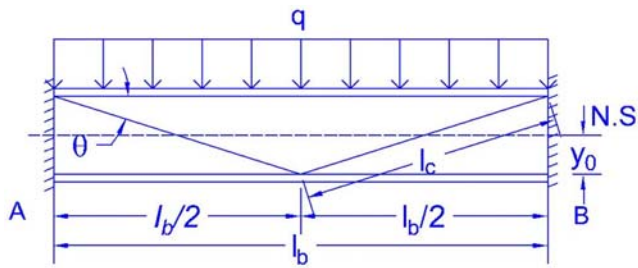


**Figure 2.5** The beam with fixed supports and the V-shaped cable pattern.

$$U = 2\times\frac{1}{2(EI)_b}\left\{\begin{array}{c}\int_0^a\left(-M+\Delta F cos\theta y_0-\left(\Delta F sin\theta-\frac{ql_b}{2}\right)x-\frac{qx^2}{2}\right)^2dx\\ +\int_a^{\frac{l_b}{2}}\left(-M-\Delta F cos\theta y_0+\frac{ql_bx}{2}-\frac{qx^2}{2}\right)^2dx\end{array}\right\}$$
$$+2\times\frac{\Delta F^2 l_c}{2(AE)_c}+\frac{(\Delta F cos\theta)^2(l_b-2a)}{2(AE)_c}+\frac{(\Delta F cos\theta)^2 l_b}{2(AE)_b}$$
$$=\frac{1}{(EI)_b}\left\{\begin{array}{c}\frac{q^2l_b^5}{240}+\frac{\Delta F^2a^3sin^2\theta}{3}+\frac{\Delta F^2l_by_0^2cos^2\theta}{2}-\Delta F^2y_0a^2sin\theta cos\theta+\frac{q\Delta Fa^4sin\theta}{4}\\ -\frac{q\Delta Fl_ba^3sin\theta}{3}-\frac{2q\Delta Fy_0a^3cos\theta}{3}+q\Delta Fl_by_0a^2cos\theta-\frac{q\Delta Fl_b^3y_0cos\theta}{12}\\ +M\Delta Fa^2sin\theta-4M\Delta Fy_0acos\theta+M\Delta Fl_by_0cos\theta-\frac{qMl_b^3}{12}+\frac{M^2l_b}{2}\end{array}\right\}$$
$$+\frac{\Delta F^2l_c}{(AE)_c}+\frac{\Delta F^2(l_b-2a)cos^2\theta}{2(AE)_c}+\frac{\Delta F^2l_bcos^2\theta}{2(AE)_b} \tag{2.19}$$

Using the least work method, the fixed end moment ($M$) and the increment of the cable's pretensioning force ($\Delta F$) are obtained as below [20]:

$$M=\frac{ql_b^2}{12}-\frac{\Delta Fa^2sin\theta}{l_b}+\frac{4\Delta Fy_0acos\theta}{l_b}-\Delta Fy_0cos\theta \tag{2.20}$$

$$\Delta F=\frac{-3ql_ba^4sin\theta+4ql_b^2a^3sin\theta-ql_b^3a^2sin\theta+8ql_by_0a^3cos\theta-12ql_b^2y_0a^2cos\theta+4ql_b^3y_0acos\theta}{4\left(\begin{array}{c}-3a^4sin^2\theta+2l_ba^3sin^2\theta-48y_0^2a^2cos^2\theta+24l_by_0^2acos^2\theta+24y_0a^3sin\theta cos\theta\\ -12l_by_0a^2sin\theta cos\theta+\frac{3l_b(EI)_b}{(AE)_c}\left[2l_c+(l_b-2a)cos^2\theta\right]+\frac{3I_bl_b^2cos^2\theta}{A_b}\end{array}\right)} \tag{2.21}$$

In Eq. (2.21), if the length of horizontal cable ($l_b-2a$, presented in Fig. 2.6) moved toward zero, Eq. (2.16) would be acquired related to the V-shaped cable pattern.

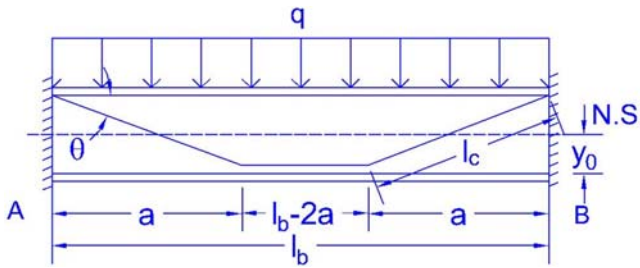


**Figure 2.6** The beam with fixed supports and the modified V-shaped cable pattern.

### 2.3.6 The beam with fixed supports and two V-shaped cable patterns

In the beam with fixed supports and two V-shaped cable patterns (Fig. 2.7), the increment of the pretensioning force in the cable equals $\Delta F$ in the first inclined part ($C_1$) and equals $\frac{\Delta F cos\theta_1}{cos\theta_2}$ in the second inclined part ($C_2$) to maintain a constant bending moment at the cable inclination change region. Accordingly, the axial force of the beam equals $2\Delta F cos\theta_1$. Furthermore, the beam with fixed supports and two V-shaped cable patterns has two degrees of indeterminacy (the increment in the pretensioning force of the cable, ΔF, and the fixed end moment, $M$). Therefore the bending moment for half of the beam with fixed supports and two V-shaped cable patterns subjected to a uniform distributed loading is obtained as below [21] to determine the total strain energy:

For $0 \le x \le a$ range,

$$M_1(x) = -M + 2\Delta F cos\theta_1 y_0 - \left(\Delta F sin\theta_1 + \Delta F cos\theta_1 tan\theta_2 - \frac{ql_b}{2}\right)x - \frac{qx^2}{2} \quad (2.22)$$

For $a \le x \le \frac{l_b}{2}$ range,

$$M_2(x) = -M - \Delta F cos\theta_1 tan\theta_2 a + \frac{ql_b x}{2} - \frac{qx^2}{2} \quad (2.23)$$

Because the structure and the loading both are symmetric, the total strain energy is determined using the relation as below:

$$\begin{aligned} U = 2 \times \frac{1}{2(EI)_b} & \left\{ \begin{array}{c} \int_0^a \left(-M + 2\Delta F cos\theta_1 y_0 - \left(\Delta F sin\theta_1 + \Delta F cos\theta_1 tan\theta_2 - \frac{ql_b}{2}\right)x - \frac{qx^2}{2}\right)^2 dx \\ + \int_a^{\frac{l_b}{2}} \left(-M - \Delta F cos\theta_1 tan\theta_2 a + \frac{ql_b x}{2} - \frac{qx^2}{2}\right)^2 dx \end{array} \right\} \\ & + 2 \times \frac{\Delta F^2 l_{c1}}{2(AE)_c} + 2 \times \frac{\left(\frac{\Delta F cos\theta_1}{cos\theta_2}\right)^2 l_{c2}}{2(AE)_c} + \frac{(2\Delta F cos\theta_1)^2 l_b}{2(AE)_b} \\ = \frac{1}{(EI)_b} & \left\{ \begin{array}{c} \frac{q^2 l_b^5}{240} + \frac{M^2 l_b}{2} + \frac{q\Delta F l_b a^3 cos\theta_1 tan\theta_2}{6} + q\Delta F l_b y_0 a^2 cos\theta_1 \\ -\frac{q\Delta F l_b^3 a cos\theta_1 tan\theta_2}{12} + \Delta F M l_b a cos\theta_1 tan\theta_2 - \frac{2\Delta F^2 a^3 cos^2\theta_1 tan^2\theta_2}{3} \\ + \Delta F M a^2 sin\theta_1 + 4\Delta F^2 y_0^2 a cos^2\theta_1 + \frac{q\Delta F a^4 sin\theta_1}{4} - \frac{q\Delta F a^4 cos\theta_1 tan\theta_2}{12} \\ -\frac{2q\Delta F y_0 a^3 cos\theta_1}{3} + \frac{2\Delta F^2 a^3 sin\theta_1 cos\theta_1 tan\theta_2}{3} - \frac{q\Delta F l_b a^3 sin\theta_1}{3} \\ -\Delta F M a^2 cos\theta_1 tan\theta_2 - 2\Delta F^2 y_0 a^2 sin\theta_1 cos\theta_1 - 2\Delta F^2 y_0 a^2 cos^2\theta_1 tan\theta_2 \\ -4\Delta F M y_0 a cos\theta_1 + \frac{\Delta F^2 l_b a^2 cos^2\theta_1 tan^2\theta_2}{2} - \frac{qMl_b^3}{12} + \frac{\Delta F^2 a^3 sin^2\theta_1}{3} \end{array} \right\} \\ & + \frac{\Delta F^2 l_{c1}}{(AE)_c} + \frac{\Delta F^2 l_{c2} cos^2\theta_1}{(AE)_c cos^2\theta_2} + \frac{2\Delta F^2 l_b cos^2\theta_1}{(AE)_b} \end{aligned} \quad (2.24)$$

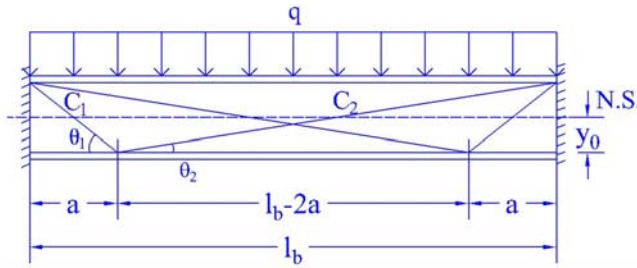


**Figure 2.7** The beam with fixed supports and two V-shaped cable patterns.

Using the least work method, the fixed end moment ($M$) and the increment of the pretensioning force in the cable, $\Delta F$, are determined as follows [21]:

$$M = \frac{ql_b^2}{12} - \Delta F a cos\theta_1 tan\theta_2 - \frac{\Delta F a^2 sin\theta_1}{l_b} + \frac{\Delta F a^2 cos\theta_1 tan\theta_2}{l_b} + \frac{4\Delta F y_0 a cos\theta_1}{l_b} \tag{2.25}$$

$$\Delta F = \frac{\begin{array}{c} -2ql_b^2 a^3 cos\theta_1 tan\theta_2 - 12ql_b^2 y_0 a^2 cos\theta_1 - ql_b^3 a^2 sin\theta_1 - 3ql_b a^4 sin\theta_1 + ql_b a^4 cos\theta_1 tan\theta_2 \\ + 8ql_b y_0 a^3 cos\theta_1 + 4ql_b^2 a^3 sin\theta_1 + ql_b^3 a^2 cos\theta_1 tan\theta_2 + 4ql_b^3 y_0 a cos\theta_1 \end{array}}{4\left( \begin{array}{c} -2l_b a^3 sin\theta_1 cos\theta_1 tan\theta_2 + 2l_b a^3 cos^2\theta_1 tan^2\theta_2 + 12l_b y_0 a^2 cos^2\theta_1 tan\theta_2 - 3a^4 sin^2\theta_1 \\ +6a^4 sin\theta_1 cos\theta_1 tan\theta_2 + 24y_0 a^3 sin\theta_1 cos\theta_1 + 24l_b y_0^2 a cos^2\theta_1 - 3a^4 cos^2\theta_1 tan^2\theta_2 \\ - 24y_0 a^3 cos^2\theta_1 tan\theta_2 - 12l_b y_0 a^2 sin\theta_1 cos\theta_1 - 48y_0^2 a^2 cos^2\theta_1 + 2l_b a^3 sin^2\theta_1 \\ + \frac{6l_b (EI)_b}{(AE)_c}\left[ l_{c1} + \frac{l_{c2} cos^2\theta_1}{cos^2\theta_2} \right] + \frac{12 I_b l_b^2 cos^2\theta_1}{A_b} \end{array} \right)} \tag{2.26}$$

As Fig. 2.7 shows, if $sin\theta_1 = \frac{2y_0}{\sqrt{a^2 + 4y_0^2}}$, $cos\theta_1 = \frac{a}{\sqrt{a^2 + 4y_0^2}}$, and $tan\theta_2 = \frac{2y_0}{l_b - a}$ were replaced in Eq. (2.25), the fixed end moment would be equal to $\frac{ql_b^2}{12}$ related to the fixed end moment in the steel beam without cable.

### 2.3.7 The cantilever beam along with the cables

Since the steel cable inclination is constant, the increment in the pretensioning force of the cable equals $\Delta F$ in the cantilever beam along with the cables (Fig. 2.8). Accordingly, the axial force of the beam equals $\Delta F \cos\theta$. Therefore the bending moment of the cantilever beam along with the cables under uniform distributed loading is achieved by the following relation [22] to calculate the total strain energy.

For $0 \le x \le l_b$ range,

$$M(x) = \Delta F cos\theta y_0 - \frac{ql_b^2}{2} - (\Delta F sin\theta - ql_b)x - \frac{qx^2}{2} \tag{2.27}$$

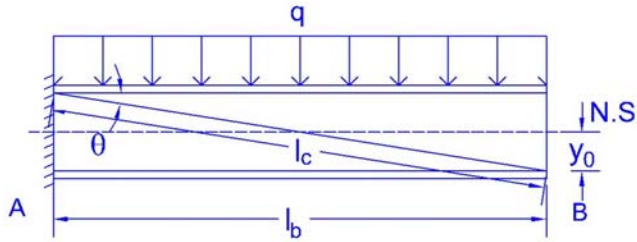


**Figure 2.8** Cantilever beam along with cables.

The total strain energy is determined through:

$$U = \frac{1}{2(EI)_b}\int_0^{l_b}\left(\Delta F cos\theta y_0 - \frac{ql_b^2}{2} - (\Delta F sin\theta - ql_b)x - \frac{qx^2}{2}\right)^2 dx + \frac{\Delta F^2 l_c}{2(AE)_c} + \frac{(\Delta F cos\theta)^2 l_b}{2(AE)_b} = \frac{1}{2(EI)_b}\left\{\begin{array}{c} \frac{q^2 l_b^5}{20} + \frac{\Delta F^2 l_b^3 sin^2\theta}{3} + \Delta F^2 l_b y_0^2 cos^2\theta \\ -\Delta F^2 l_b^2 y_0 sin\theta cos\theta + \frac{q\Delta F l_b^4 sin\theta}{12} - \frac{q\Delta F l_b^3 y_0 cos\theta}{3} \end{array}\right\} + \frac{\Delta F^2 l_c}{2(AE)_c} + \frac{\Delta F^2 l_b cos^2\theta}{2(AE)_b} \tag{2.28}$$

Using the least work method, the increase in the pretensioning force of the cable ($\Delta F$) can be determined as below [22]:

$$\Delta F = \frac{-ql_b^4 sin\theta + 4ql_b^3 y_0 cos\theta}{8\left(l_b^3 sin^2\theta + 3l_b y_0^2 cos^2\theta - 3l_b^2 y_0 sin\theta cos\theta + \frac{3(EI)_b l_c}{(AE)_c} + \frac{3I_b l_b cos^2\theta}{A_b}\right)} \tag{2.29}$$

## 2.4 Deflection

Using the method of virtual work and neglecting the effects of shear and axial force, the beams' deflection with different types of support both without cable and with different cable patterns can be determined by using the method of virtual work. Maximum deflection of the beams with simple supports, fixed supports, and cantilever beams without cable subjected to uniform distributed load $q$ with length and flexural rigidity of $l_b$ and $(El)_b$, respectively, is obtained as follows:

The maximum deflection of beams with simple supports without cable:

$$\Delta_{mid} = \frac{5ql_b^4}{384(EI)_b} \tag{2.30}$$

The maximum deflection of beams with fixed supports without cable:

$$\Delta_{mid} = \frac{ql_b^4}{384(EI)_b} \tag{2.31}$$

The maximum deflection of cantilever beams without cable:

$$\Delta_{end} = \frac{ql_b^4}{8(EI)_b} \tag{2.32}$$

### 2.4.1 Maximum deflection of the beam with simple supports and the V-shaped cable pattern

Due to the existed symmetry in the structure and loading (as presented in Fig. 2.2), the bending moment for half of the beams with simple supports and the V-shaped cable pattern subjected to real loading with the cable force equal to $F$ is calculated as follows [20]:

For $0 \leq x \leq \frac{l_b}{2}$ range:

$$M(x) = Fcos\theta y_0 - \left(Fsin\theta - \frac{ql_b}{2}\right)x - \frac{qx^2}{2} \tag{2.33}$$

where $F = F_{pt} + \Delta F$ presents the total cable force; $F_{pt}$ is used for the initial pretensioning force of the cable; and $\Delta F$ shows the increment of the pretensioning force in the cable.

In the analysis of the structure subjected to virtual loading, the constraints can be omitted to make a stable determinate structure in case the system was indeterminate. In the system of beam and cable, the cable is a redundant constraint. Therefore it can be removed. Thus the bending moment for half of the beams with simple supports under virtual loading (Fig. 2.9) is calculated as follows:

For $0 \leq x \leq \frac{l_b}{2}$ range:

$$m(x) = \frac{x}{2} \tag{2.34}$$

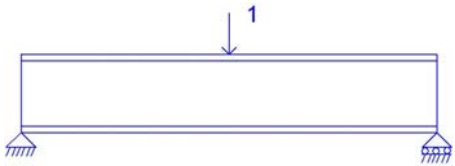


**Figure 2.9** Simply supported beam under virtual loading.

Using the method of virtual work, the maximum deflection of the simply supported beam along with the V-shaped cable pattern is obtained through [20] as below:

$$1 \times \Delta = \int \frac{M(x)m(x)}{EI}dx = \frac{2}{(EI)_b}\int_0^{\frac{l_b}{2}} \left(Fcos\theta y_0 - (Fsin\theta - \frac{ql_b}{2})x - \frac{qx^2}{2}\right)\left(\frac{x}{2}\right)dx$$
$$= \frac{1}{(EI)_b}\left[\frac{5ql_b^4}{384} - \frac{Fl_b^3 sin\theta}{24} + \frac{Fl_b^2 y_0 cos\theta}{8}\right] \tag{2.35}$$

### 2.4.2 Maximum deflection of the beam with simple supports and the modified V-shaped cable pattern

Due to the existed symmetry in the structure and loading (as presented in Fig. 2.3), if the cable force was equal to $F$ in the inclined parts and equal to $Fcos\theta$ in the horizontal part, the bending moment for half of the beam with simple supports and the modified V-shaped cable pattern subjected to a real loading is calculated through [20] as below:

For $0 \leq x \leq$ a range,

$$M_1(x) = Fcos\theta y_0 - \left(Fsin\theta - \frac{ql_b}{2}\right)x - \frac{qx^2}{2} \tag{2.36}$$

For a $\leq x \leq \frac{l_b}{2}$ range:

$$M_2(x) = -Fcos\theta y_0 + \frac{ql_b x}{2} - \frac{qx^2}{2} \tag{2.37}$$

Using the virtual work method, the maximum deflection of the beam with simple supports and the modified V-shaped cable pattern is calculated using Eq. (2.34) as follows [20]:

$$1 \times \Delta = \int \frac{M(x)m(x)}{EI}dx = \frac{2}{(EI)_b}\left[\begin{array}{l}\int_0^a \left(Fcos\theta y_0 - (Fsin\theta - \frac{ql_b}{2})x - \frac{qx^2}{2}\right)\left(\frac{x}{2}\right)dx \\ + \int_a^{\frac{l_b}{2}} \left(-Fcos\theta y_0 + \frac{ql_b x}{2} - \frac{qx^2}{2}\right)\left(\frac{x}{2}\right)dx\end{array}\right]$$
$$= \frac{1}{(EI)_b}\left[\frac{5ql_b^4}{384} - \frac{Fa^3 sin\theta}{3} + Fy_0 a^2 cos\theta - \frac{Fl_b^2 y_0 cos\theta}{8}\right] \tag{2.38}$$

In Eq. (2.38), if the length of horizontal cable ($l_b - 2a$, as observed in Fig. 2.3) moved toward zero, Eq. (2.35) would be acquired related to the V-shaped cable pattern.

### 2.4.3 Maximum deflection of the beam with simple supports and two V-shaped cable patterns

Because the structure and the loading both are symmetric (as demonstrated in Fig. 2.4), if the cable force was equal to $F$ in the first inclined part ($C_1$) and equal to $\frac{Fcos\theta_1}{cos\theta_2}$ in the second inclined part ($C_2$), the bending moment for half of the beam with simple supports and two V-shaped cable patterns subjected to a real loading would be calculated through [21] as below:

For $0 \le x \le a$ range,

$$M_1(x) = 2Fcos\theta_1 y_0 - \left(Fsin\theta_1 + Fcos\theta_1 tan\theta_2 - \frac{ql_b}{2}\right)x - \frac{qx^2}{2} \tag{2.39}$$

For $a \le x \le \frac{l_b}{2}$ range,

$$M_2(x) = -Fcos\theta_1 tan\theta_2 a + \frac{ql_b x}{2} - \frac{qx^2}{2} \tag{2.40}$$

Using the virtual work method, the maximum deflection of the beam with simple supports and two V-shaped cable patterns is determined using Eq. (2.34) as follows [21]:

$$\begin{aligned} 1 \times \Delta = \int \frac{M(x)m(x)}{EI}dx &= \frac{2}{(EI)_b}\left[\int_0^a \left(2Fcos\theta_1 y_0 - (Fsin\theta_1 + Fcos\theta_1 tan\theta_2 - \frac{ql_b}{2})x - \frac{qx^2}{2}\right)\left(\frac{x}{2}\right)dx \right. \\ &\left. + \int_a^{\frac{l_b}{2}} \left(-Fcos\theta_1 tan\theta_2 a + \frac{ql_b x}{2} - \frac{qx^2}{2}\right)\left(\frac{x}{2}\right)dx\right] \\ &= \frac{1}{(EI)_b}\left[\frac{5ql_b^4}{384} - \frac{Fa^3 sin\theta_1}{3} + \frac{Fa^3 cos\theta_1 tan\theta_2}{6} + Fy_0 a^2 cos\theta_1 - \frac{Fl_b^2 acos\theta_1 tan\theta_2}{8}\right] \end{aligned} \tag{2.41}$$

### 2.4.4 Maximum deflection of the beam with fixed supports and the V-shaped cable pattern

Due to the symmetry of the structure and loading (as showed in Fig. 2.5), if the cable force was equal to $F$, and the fixed end moment ($M$) was equal to $\frac{ql_b^2}{12}$, the bending moment for half of the beam with fixed supports and the V-shaped cable pattern subjected to real loading could be obtained as below [20]:

For $0 \leq x \leq \frac{l_b}{2}$ range,

$$\begin{aligned} M(x) &= -M + F\cos\theta y_0 - \left(F\sin\theta - \frac{ql_b}{2}\right)x - \frac{qx^2}{2} \\ &= -\frac{ql_b^2}{12} + F\cos\theta y_0 - \left(F\sin\theta - \frac{ql_b}{2}\right)x - \frac{qx^2}{2} \end{aligned} \tag{2.42}$$

The bending moment for half of the beam with fixed supports subjected to a virtual loading (Fig. 2.10) is calculated as follows:

For $0 \leq x \leq \frac{l_b}{2}$ range,

$$m(x) = \frac{x}{2} - \frac{l_b}{8} \tag{2.43}$$

Using the virtual work method, the maximum deflection of the beam with fixed supports and the V-shaped cable pattern is calculated using Eq. (2.43) as follows [20]:

$$\begin{aligned} 1 \times \Delta &= \int \frac{M(x)m(x)}{EI}dx = \frac{2}{(EI)_b}\int_0^{\frac{l_b}{2}} \left(-\frac{ql_b^2}{12} + F\cos\theta y_0 - (F\sin\theta - \frac{ql_b}{2})x - \frac{qx^2}{2}\right)\left(\frac{x}{2} - \frac{l_b}{8}\right)dx \\ &= \frac{1}{(EI)_b}\left[\frac{ql_b^4}{384} - \frac{Fl_b^3\sin\theta}{96}\right] \end{aligned} \tag{2.44}$$

### 2.4.5 Maximum deflection of the beam with fixed supports and the modified V-shaped cable pattern

If the cable force equals $F$ in the inclined part and equals $F\cos\theta$ in the horizontal part, the fixed end moment ($M$) is determined by the following relation (as displayed in Section 2.3.5):

$$M = \frac{ql_b^2}{12} - \frac{Fa^2\sin\theta}{l_b} + \frac{4Fy_0a\cos\theta}{l_b} - Fy_0\cos\theta \tag{2.45}$$

Because both the structure and the loading are symmetric (Fig. 2.6), the bending moment for half of the beam with fixed supports and the modified V-shaped cable pattern subjected to a real loading is calculated through [20] as below:

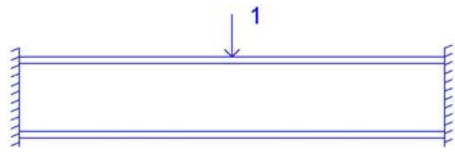


**Figure 2.10** Fixed supported beam under virtual loading.

For $0 \le x \le a$ range,

$$M_1(x) = -M + Fcos\theta y_0 - \left(Fsin\theta - \frac{ql_b}{2}\right)x - \frac{qx^2}{2}$$
$$= -\frac{ql_b^2}{12} + \frac{Fa^2 sin\theta}{l_b} - \frac{4Fy_0 acos\theta}{l_b} + 2Fcos\theta y_0 - \left(Fsin\theta - \frac{ql_b}{2}\right)x - \frac{qx^2}{2} \tag{2.46}$$

For $a \le x \le \frac{l_b}{2}$ range,

$$M_2(x) = -M - Fcos\theta y_0 + \frac{ql_b x}{2} - \frac{qx^2}{2} = -\frac{ql_b^2}{12} + \frac{Fa^2 sin\theta}{l_b} - \frac{4Fy_0 acos\theta}{l_b} + \frac{ql_b x}{2} - \frac{qx^2}{2} \tag{2.47}$$

Employing the virtual work method, the maximum deflection of the beam with fixed supports and the modified V-shaped cable pattern is obtained using Eq. (2.43) as follows [20]:

$$1 \times \Delta = \int \frac{M(x)m(x)}{EI}dx = \frac{2}{(EI)_b}\left(\int_0^a \left(\begin{array}{c} -\frac{ql_b^2}{12} + \frac{Fa^2 sin\theta}{l_b} - \frac{4Fy_0 acos\theta}{l_b} + 2Fcos\theta y_0 \\ -\left(Fsin\theta - \frac{ql_b}{2}\right)x - \frac{qx^2}{2} \end{array}\right)\left(\frac{x}{2} - \frac{l_b}{8}\right)dx + \int_a^{\frac{l_b}{2}} \left(\begin{array}{c} -\frac{ql_b^2}{12} + \frac{Fa^2 sin\theta}{l_b} \\ -\frac{4Fy_0 acos\theta}{l_b} + \frac{ql_b x}{2} - \frac{qx^2}{2} \end{array}\right)\left(\frac{x}{2} - \frac{l_b}{8}\right)dx\right)$$
$$= \frac{1}{(EI)_b}\left[\frac{ql_b^4}{384} - \frac{Fa^3 sin\theta}{3} + \frac{Fl_b a^2 sin\theta}{8} + F_{y_0}a^2 cos\theta - \frac{Fl_b y_0 acos\theta}{2}\right] \tag{2.48}$$

In Eq. (2.48), if the length of horizontal cable ($l_b - 2a$, as observed in Fig. 2.6) approached zero, Eq. (2.44) would be acquired related to the V-shaped cable pattern.

### 2.4.6 Maximum deflection of the beam with fixed supports and two V-shaped cable patterns

Due to the existed symmetry in the structure and loading (as presented in Fig. 2.7), if the cable force was equal to $F$ in the first inclined part ($C_1$) and was equal to $\frac{Fcos\theta_1}{cos\theta_2}$ in the second inclined part ($C_2$), and the fixed end moment ($M$) was equal to

$\frac{ql_b^2}{12}$, the bending moment for half of the beam with fixed supports and two V-shaped cable patterns subjected to real loading could be calculated through [21] as below:

For $0 \leq x \leq a$ range:

$$\begin{aligned} M_1(x) &= -M + 2Fcos\theta_1 y_0 - \left(Fsin\theta_1 + Fcos\theta_1 tan\theta_2 - \frac{ql_b}{2}\right)x - \frac{qx^2}{2} \\ &= -\frac{ql_b^2}{12} + 2Fcos\theta_1 y_0 - \left(Fsin\theta_1 + Fcos\theta_1 tan\theta_2 - \frac{ql_b}{2}\right)x - \frac{qx^2}{2} \end{aligned} \tag{2.49}$$

For $a \leq x \leq \frac{l_b}{2}$ range,

$$\begin{aligned} M_2(x) &= -M - Fcos\theta_1 tan\theta_2 a + \frac{ql_b x}{2} - \frac{qx^2}{2} \\ &= -\frac{ql_b^2}{12} - Fcos\theta_1 tan\theta_2 a + \frac{ql_b x}{2} - \frac{qx^2}{2} \end{aligned} \tag{2.50}$$

Utilizing the virtual work method, the maximum deflection of the beam with fixed supports and two V-shaped cable patterns is obtained using Eq. (2.43) as follows [21]:

$$\begin{aligned} 1 \times \Delta &= \int \frac{M(x)m(x)}{EI}dx \\ &= \frac{2}{(EI)_b}\left(\begin{array}{c} \int_0^a \left(-\frac{ql_b^2}{12} + 2Fcos\theta_1 y_0 - \left(Fsin\theta_1 + Fcos\theta_1 tan\theta_2 - \frac{ql_b}{2}\right)x - \frac{qx^2}{2}\right)\left(\frac{x}{2} - \frac{l_b}{8}\right)dx \\ + \int_a^{\frac{l_b}{2}} \left(-\frac{ql_b^2}{12} - Fcos\theta_1 tan\theta_2 a + \frac{ql_b x}{2} - \frac{qx^2}{2}\right)\left(\frac{x}{2} - \frac{l_b}{8}\right)dx \end{array}\right) \\ &= \frac{1}{(EI)_b}\left(\begin{array}{c} \frac{ql_b^4}{384} + Fy_0 a^2 cos\theta_1 + \frac{Fa^3 cos\theta_1 tan\theta_2}{6} + \frac{Fl_b a^2 sin\theta_1}{8} - \frac{Fl_b a^2 cos\theta_1 tan\theta_2}{8} \\ - \frac{Fl_b y_0 a cos\theta_1}{2} - \frac{Fa^3 sin\theta_1}{3} \end{array}\right) \end{aligned} \tag{2.51}$$

### 2.4.7 Maximum deflection of cantilever beam along with cables

If the cable force was equal to $F$, the bending moment for the cantilever beam along with cables under real loading would be calculated as follows [22]:


**Figure 2.11** Cantilever beam under virtual loading.

For $0 \leq x \leq l_b$ range,

$$M(x) = -\frac{ql_b^2}{2} + Fcos\theta y_0 - \left(Fsin\theta - ql_b\right)x - \frac{qx^2}{2} \tag{2.52}$$

The bending moment for the cantilever beam under virtual loading (Fig. 2.11) is calculated as follows:

For $0 \leq x \leq l_b$ range,

$$M(x) = \mathrm{x} - l_b \tag{2.53}$$

Using the method of virtual work, the maximum deflection of the cantilever beam along with cables can be obtained using Eq. (2.53) as follows [22]:

$$1 \times \Delta = \int \frac{M(x)m(x)}{EI}dx = \frac{1}{(EI)_b}\int_0^{l_b}\left(-\frac{ql_b^2}{2} + Fcos\theta y_0 - (Fsin\theta - ql_b)x - \frac{qx^2}{2}\right)(x - l_b)dx$$
$$= \frac{1}{(EI)_b}\left[\frac{ql_b^4}{8} + \frac{Fl_b^3 sin\theta}{6} - \frac{Fl_b^2 y_0 cos\theta}{2}\right] \tag{2.54}$$

## 2.5 Finite element modeling of I-shaped symmetric pretensioned steel beams with steel cables

Using the method of load and resistance factor design, the beams with simple supports, fixed supports, and cantilever beams were designed using AISC360−10 code [26]. The maximum deflections of the beam with simple supports and cantilever beams subjected to dead load and live load exceed the allowable range ($\frac{1}{240}$ of the beam length). However, the maximum deflection of the fixed supported beam meets the code's limitation because of the high stiffness. Therefore the beam with fixed supports was considered to investigate the cable's effects. Table 2.1 presents the properties of the simply supported, fixed supported, and cantilever beams. It is momentous to be mentioned that the loading span is 1.5 m long, and the dead load and live load are 450 and 200 kg $m^{-2}$, respectively [20−22].

**Table 2.1** Properties of beams with various support conditions.

| Type of beam | Cross section of the beam | Span length (m) | Maximum deflection (cm) | Allowable deflection (cm) |
|---|---|---|---|---|
| Simply supported beam | IPE400 | 12 | 5.691 | 5 |
| Fixed supported beam | IPE330 | 12 | 2.237 | 5 |
| Cantilever beam | IPB120 | 2 | 1.128 | 0.833 |

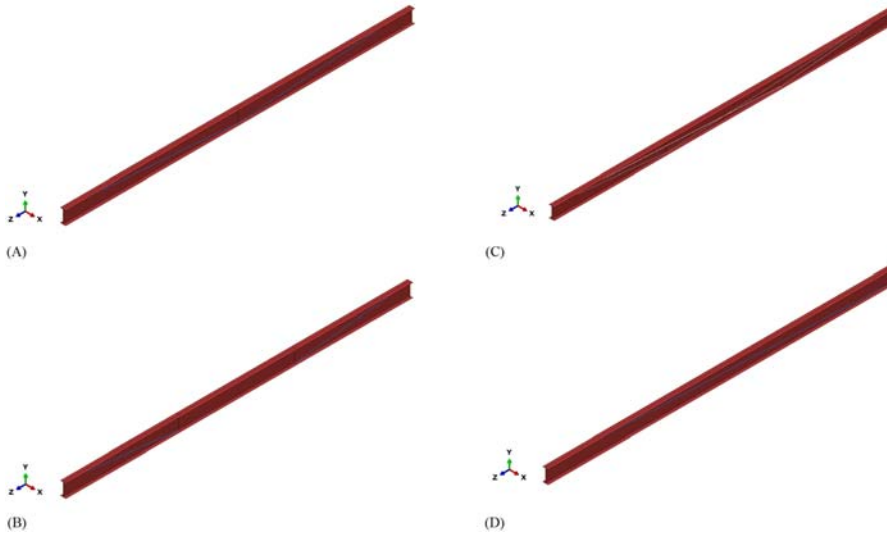


**Figure 2.12** Finite element models: (A) the beam with simple or fixed supports with the V-shaped cable pattern; (B) the beam with simple or fixed supports with the modified V-shaped cable pattern; (C) the beam with simple or fixed supports with two V-shaped cable patterns; (D) the cantilever beam along with the cables.

As Fig. 2.12 shows, the simply supported, fixed supported, and cantilever beams with different cable patterns subjected to uniform distributed loading are modeled employing the Abaqus FE software. The shell and truss elements are used to model the beams and cables, respectively, in three-dimensional space. The weld's connector provided a perfect connection between the cable and the top flange of the beam nodes. Besides, the coupling constraint is employed to model the behavior of the deviator. The uniform distributed loading and the cable's pretensioning initial force applied to the models using the surface

traction type and predefined field tool, respectively. Furthermore, static general assessment of Abaqus FE software is employed to evaluate the systems of beam and cable. Fig. 2.13 represents the cables' locations in the beams with various support conditions [20–22].

The results of the modeling of steel beams without cable and with various cable patterns are compared with each other to investigate the behavior of the systems of beam and cable. The beams' material is steel ST-37 with yield stress of 240 MPa, elasticity modulus of 200 GPa, Poisson's ratio of 0.3, and density of 7850 kg $m^{-3}$. The steel cable's material is determined based on ASTM A416M standard [27]. 7-wire strand [grade 270 (1860)] is regarded for the steel cable with low relaxation, minimum ultimate strength ($f_{pu}$) of 270 ksi (1860 MPa), minimum yield strength at

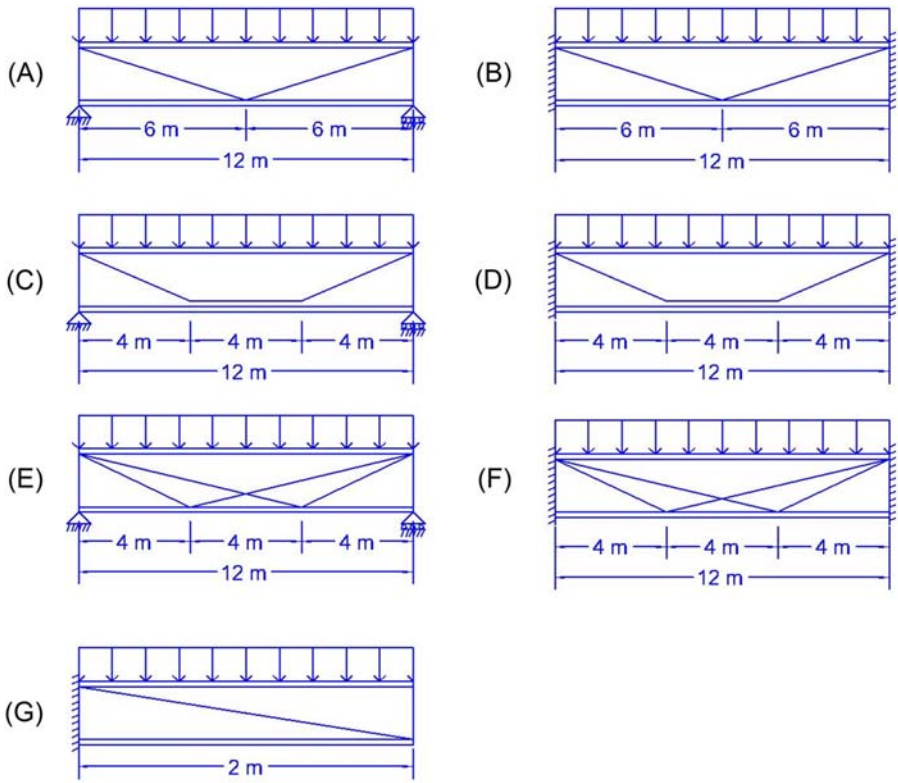


**Figure 2.13** The locations of cables in the beams: (A) the beam with simple supports and the V-shaped cable pattern; (B) the beam with simple supports and the modified V-shaped cable pattern; (C) the beam with simple supports and two V-shaped cable patterns; (D) the beam with fixed supports and the V-shaped cable pattern; (E) the beam with fixed supports and the modified V-shaped cable pattern; (F) the beam with fixed supports and two V-shaped cable patterns; (G) the cantilever beam along with the cables.

**Table 2.2** Cross-sectional area of cables for beams with different types of supports.

| Type of beam | Simply supported beam | Fixed supported beam | Cantilever beam |
|---|---|---|---|
| Total cross-sectional area of steel cable ($mm^2$) | 560 | 395 | 297 |

1% extension of 52.74 kip (234.6 kN), elasticity modulus of $28.5 \times 10^6$ psi (196501.8 MPa), and Poisson's ratio of 0.3 [20−22].

Since the horizontal component of the cable force produces axial forces in steel beams, they are designed as beam-columns based on AISC360−10 code to consider simultaneous effects of axial force and bending moment. It should be noted that the lateral braces are considered to prevent the beam from buckling about the longitudinal axis [20−22].

## 2.6 Calibration of theoretical relations with numerical models

Based on the ASTM A416 standard, the cross-sectional areas of the steel cables are considered as presented in Table 2.2. Moreover, the initial pretensioning stress of the cable is 600 MPa. Therefore the maximum deflections of the beams with simple and fixed supports, and the cantilever beam with and without various cable patterns acquired from numerical models are compared to those of theoretical equations in Table 2.3 [20−22] to validate the theoretical relations.

The beam haunch cannot be modeled because the beam was modeled as shell elements in Abaqus FE software. Therefore, as Table 2.3 presents, the maximum deflections of the beam without cable acquired from numerical models are to some extent more than those resulted from theoretical relations. As a result, reducing the moment of inertia of beam sections in the numerical models increases the maximum deflections of the beams without cables. Besides, the beams' maximum deflections along with different cable patterns acquired from numerical models are very close to the results from theoretical relations. In fact, in the numerical models, the errors, which occurred while calculating the maximum deflection of the beams along with different cable patterns related to the increase of the pretensioning force in the cable and the maximum deflection of the beams without cables caused by the uniform distributed loading, neutralize the effects of each other. It should be noted that the cable force causes a bending moment in the opposite direction of the bending moment caused by the uniform distributed loading. Therefore the beams' maximum deflections with varying conditions of support compared to the beams without cables are reduced by using different cable patterns and lead to satisfying the code's allowable limit. Based on the obtained results (as presented in Table 2.3), the most

**Table 2.3** Maximum deflections acquired from numerical models and theoretical relations.

| **Type of beam** | | **Maximum deflection of beam calculated by modeling (cm)** | **Maximum deflection of beam calculated by theoretical equations (cm)** | **Allowable deflection (cm)** |
|---|---|---|---|---|
| Simply supported beam | Without cable | 5.877 | 5.691 | 5 |
| | With V-shaped cable pattern | 4.898 | 4.851 | |
| | With modified V-shaped cable pattern | 3.768 | 3.833 | |
| | With two V-shaped cable patterns | 4.270 | 4.302 | |
| Fixed supported beam | Without cable | 2.381 | 2.237 | 5 |
| | With V-shaped cable pattern | 1.253 | 1.258 | |
| | With modified V-shaped cable pattern | 1.122 | 1.140 | |
| | With two V-shaped cable patterns | 0.521 | 0.622 | |
| Cantilever beam | Without cable | 1.151 | 1.128 | 0.833 |
| | With cable | 0.685 | 0.783 | |

appropriate cable patterns for reducing the maximum deflection are the modified V-shaped cable pattern, and two V-shaped cable patterns in the beams with simple and fixed supports, respectively [20–22].

## 2.7 The effects of horizontal cable length on the maximum deflections of the beams with simple and fixed supports with the modified V-shaped cable pattern

Figs. 2.14 and 2.15 show the maximum deflections in the beams with simple and fixed supports with the modified V-shaped cable pattern. The deflections are plotted based on the horizontal cable length ($l_b - 2a$, as observed in Figs. 2.3 and 2.6) according to Eqs. (2.38) and (2.48), Table 2.1 for the cross section of the beams with simple and fixed supports, and Table 2.2 for the cross section of steel cable [20].

As Figs. 2.14 and 2.15 show, when the horizontal cable lengths ($l_b - 2a$, as observed in Figs. 2.3 and 2.6) are zero, the maximum deflections of the beams with simple and fixed supports with the modified V-shaped cable pattern equal 4.851 and 1.258 cm, respectively, related to the V-shaped cable pattern in Table 2.3. By increasing the horizontal cable length, the maximum deflections reduce. Finally, the maximum deflections in the beams with simple and fixed supports with the modified V-shaped cable pattern for the horizontal cable lengths of 9.4 and 3 m are minimums as 3.121 and 1.127 cm, respectively. As the horizontal cable lengths increase, the maximum deflections increase as well. When the horizontal cable lengths equal beam lengths, the maximum deflections of the beams with simple and fixed supports with the modified V-shaped cable pattern equal 5.691 and 2.237 cm, respectively, related to the beams without cables in Table 2.3.

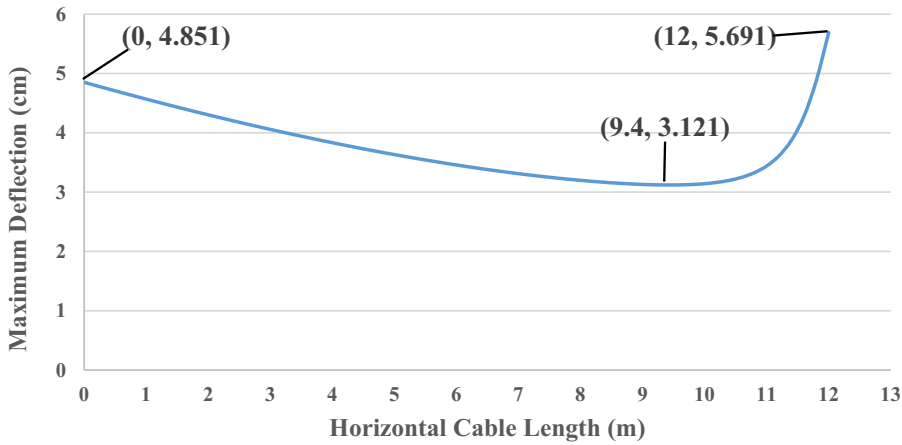


**Figure 2.14** Maximum deflections of the beam with simple supports and the modified V-shaped cable pattern for various horizontal cable lengths.

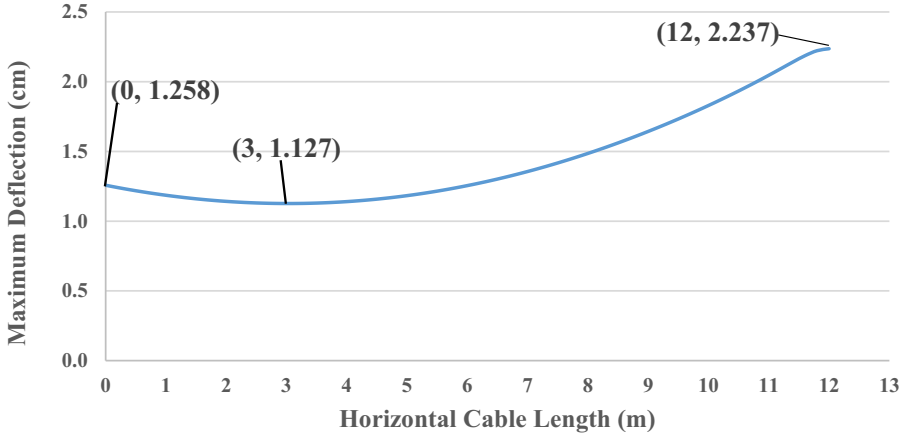


**Figure 2.15** Maximum deflections of the beam with fixed supports and the modified V-shaped cable pattern for various horizontal cable lengths.

The explanation is that the force of the horizontal cable should equal the horizontal component of the inclined cable force to maintain a constant amount of bending moment at the cable inclination change region. Hence, in this particular condition, when the horizontal component of the vertical cable force equals zero, the horizontal cable force equals zero as well. Furthermore, since the length of the vertical cable (the distance between two flanges of the beam) remains constant, no force is produced in the length of the cable. Generally, it can be concluded that when the length of the horizontal cable equals beam length, the cable does not have any influence on the behavior of the beam. Therefore the maximum deflection of the beam without cables is obtained [20].

## 2.8 The effects of length a on the maximum deflections of the beams with simple and fixed supports with two V-shaped cable patterns

In Figs. 2.16 and 2.17, the maximum deflections of the beams with simple and fixed supports with two V-shaped cable patterns are plotted based on the length $a$, as showed in Figs. 2.4 and 2.7, for half of the beam according to Eqs. (2.41) and (2.51), Table 2.1 for the cross section of the beams with simple and fixed supports, and Table 2.2 for the steel cable's cross section [21].

As shown in Figs. 2.16 and 2.17, when the length $a$ (as observed in Figs. 2.4 and 2.7) is zero, the maximum deflections of the beams with simple and fixed supports with two V-shaped cable patterns equal 5.691 and 2.237 cm, respectively, related to the beams without cables in Table 2.3 (the reason was explained in Section 2.7). Finally, when the length a equals half-length of the beam, the maximum deflections of the beams with simple and fixed supports with two V-shaped cable patterns are minimums of 4.016 and 0.286 cm, respectively [21].

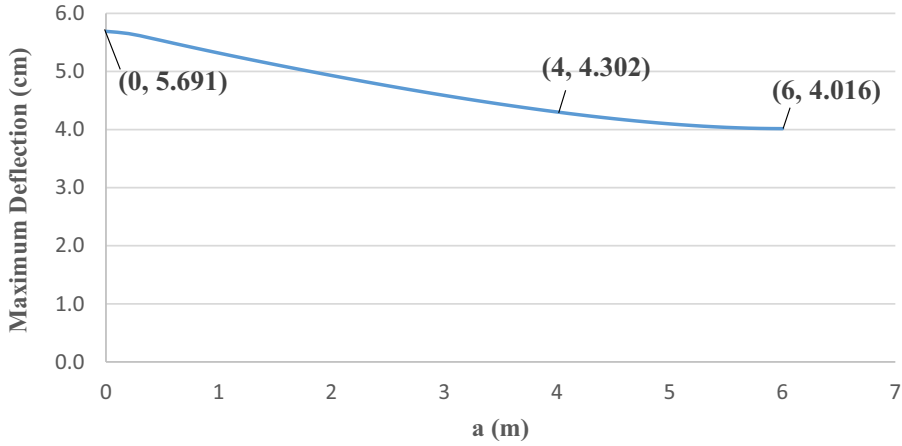


**Figure 2.16** Maximum deflections of the beams with simple supports and two V-shaped cable patterns for various values of length *a*.

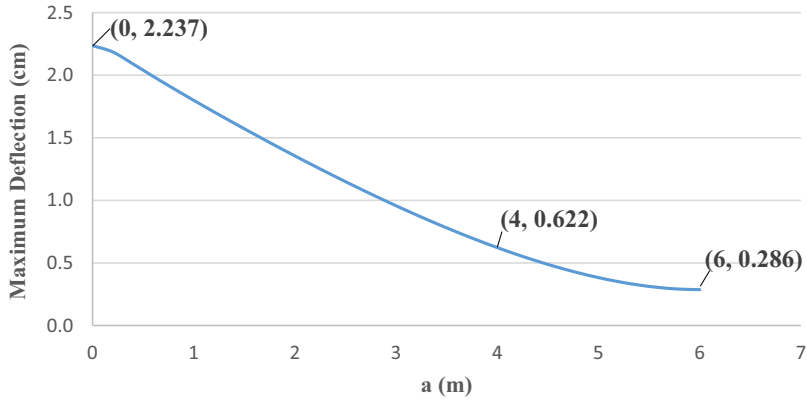


**Figure 2.17** Maximum deflections of the beams with fixed supports and two V-shaped cable patterns for various values of length *a*.

## 2.9 Comparison of bending moment diagrams of beams with and without cables

The bending moment diagrams of the simply supported, fixed supported, and cantilever beams without cable and with various cable patterns are drawn according to Table 2.1 for the cross section of simply supported and fixed supported beams and also, Table 2.2 for the cross section of steel cable. The graphs were compared with each other then. Furthermore, in those diagrams, the initial pretensioning stress of the cable is 600 MPa.

### 2.9.1 Comparison of bending moment diagrams of simply supported beams without cables and with cables

In Fig. 2.18, the diagrams of bending moments for the beams with simple supports and either without cable or with various cable patterns (V-shaped cable pattern, modified V-shaped cable pattern, and two V-shaped cable patterns) are drawn according to Eqs. (2.33), (2.36), (2.37), (2.39), and (2.40) [20,21].

As observed in Fig. 2.18, the bending moment of the beams with simple supports with various cable patterns is increased compared to those without cables from each support to the bending moment location being equal to those of beams with simple supports and without cables and then is reduced between two equivalent bending moment locations of the beams with simple supports and various cable patterns, and the beams with simple supports but without cables. Thus it is inferred that should the cables start from the neutral surface at each support, the bending moment of the beam with simple supports and various cable patterns will not increase compared to the simply supported beam without cables [20,21].

### 2.9.2 The comparison of the bending moment diagrams of the beams with fixed supports, with and without cables

In Fig. 2.19, the bending moment diagrams of the beams with fixed supports without cable and with various cable patterns (V-shaped cable pattern, modified V-shaped cable pattern, and two V-shaped cable patterns) are drawn according to Eqs. (2.42), (2.46), (2.47), (2.49), and (2.50) [20,21].

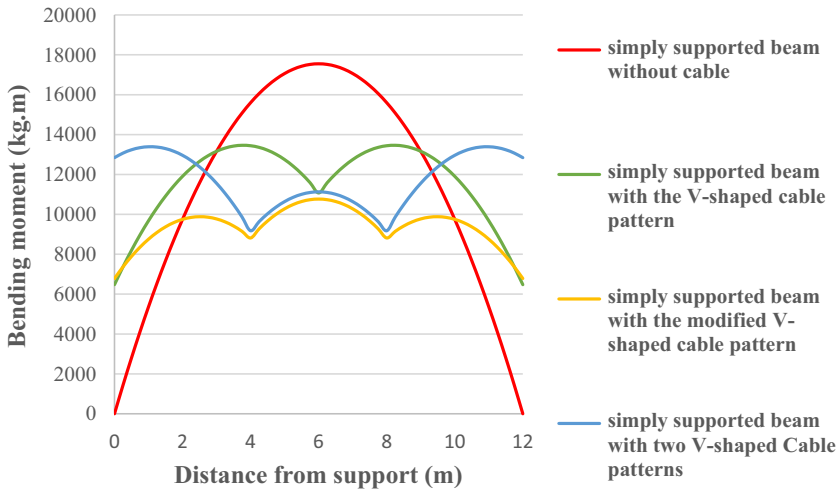


**Figure 2.18** Bending moment diagrams of the beams with simple supports either without cable or with various cable patterns.

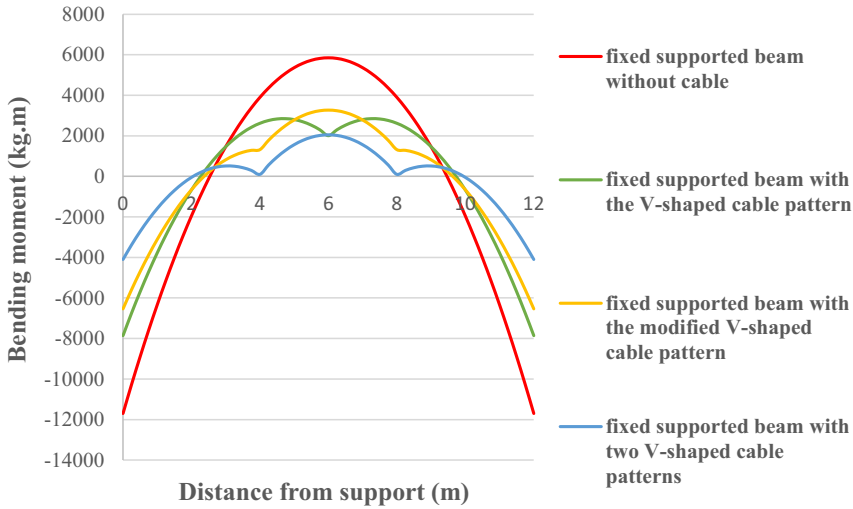


**Figure 2.19** The bending moment diagrams of the beams with fixed supports without cable and with various cable patterns.

As Fig. 2.19 presents, the bending moment of the beams with fixed supports and various cable patterns is reduced in comparison with those of fixed supported beams without cables [20,21].

### *2.9.3 The comparison of the diagrams of the bending moments of cantilever beams with and without cables*

In Fig. 2.20, the diagrams of the bending moments of cantilever beams with and without cables are drawn according to Eq. (2.52) [22].

As observed in Fig. 2.20, the bending moment of the cantilever beam with cables is reduced in comparison to that of the cantilever beam without cables from each support to the bending moment location being equal to that of cantilever beam without cables and after that is augmented. Thus it is inferred that should the cables lead to the neutral surface at the free end, the bending moment of the cantilever beam with cables will not increase in comparison to the cantilever beam without cables [22].

## 2.10 Conclusion

In this research, the steel cables are used to control the maximum deflection of long steel beams under uniform distributed loadings. In spite of proper design subjected to bending and shear the maximum deflections of the beams are not within the

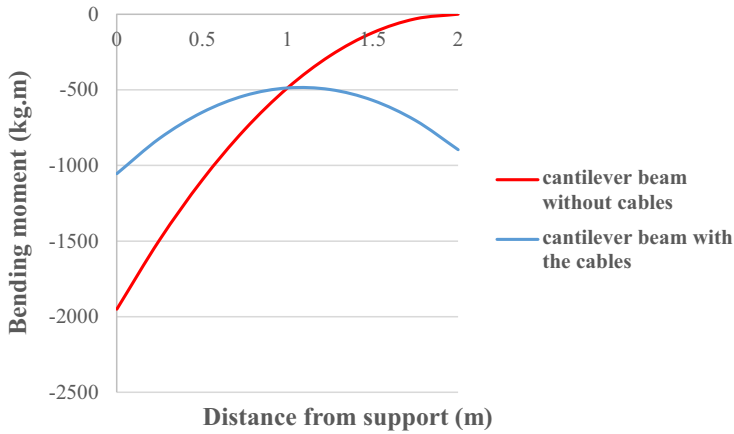


**Figure 2.20** Bending moment diagrams of cantilever beams with and without cables.

allowable range due to their distinguishing characteristics such as high tensile strength, small cross section, and low weight. The theoretical relations were derived to determine the increment of the pretensioning force in the cable and the maximum deflection in the beams with simple and fixed supports and the cantilever beam with various cable patterns. The results compared with the results of numerical models employing the Abaqus FE software. The most important results of this research can be summarized as below:

1. Although the fixed end moment ($M$) in the beams with fixed supports and the V-shaped cable pattern and two V-shaped cable patterns is equal to that of the beam without cable, ($\frac{qL_b^2}{12}$), the fixed end moment in the beam with fixed supports and the modified V-shaped cable pattern is dependent on the external loading and the total cable force.
2. Based on the results of numerical models, the theoretical equations can satisfactorily predict the maximum deflections of beams with different support conditions and cable patterns.
3. Utilizing different cable patterns reduces the beams' maximum deflections with various support conditions compared to the beams without cables and satisfies the code's allowable limit.
4. The most appropriate cable patterns to reduce the maximum deflection are the modified V-shaped cable pattern and two V-shaped cable patterns in the simply supported and fixed supported beams, respectively.
5. Based on the obtained results from the investigation of the effects of the horizontal cable lengths on the maximum deflection, when the horizontal cable lengths are zero, the maximum deflections in the beams with simple and fixed supports and the V-shaped cable pattern are acquired. By increasing the horizontal cable length, the maximum deflection is reduced. Eventually, the maximum deflections for specific horizontal cable lengths are minimum. After that, as the horizontal cable lengths increase, the maximum deflections increase too. When the horizontal cable lengths equal beam lengths, the maximum deflections in the beams with simple and fixed supports without cables are acquired.

6. Based on the obtained results from the investigation of the influences of the length $a$ on the maximum deflection, when the length $a$ is zero, the maximum deflections in the beams with simple and fixed supports without cables are acquired. Finally, when the length $a$ equals half-length of the beam, the maximum deflections in the beams with simple and fixed supports and two V-shaped cable patterns are minimums.
7. According to the bending moment diagrams, the bending moments of the simply supported, fixed supported, and cantilever beams with various cable patterns are reduced compared to those of beams without cables.

## References


[1] M. Razavi, M. Sheidaii, Seismic performance of cable zipper-braced frames, Journal of Constructional Steel Research 74 (2012) 49–57.
[2] X. Hou, H. Tagawa, Displacement-restraint bracing for seismic retrofit of steel moment frames, Journal of Constructional Steel Research 65 (5) (2009) 1096–1104.
[3] N. Fanaie, S. Aghajani, E.A. Dizaj, Theoretical assessment of the behavior of cable bracing system with central steel cylinder, Advances in Structural Engineering 19 (3) (2016) 463–472.
[4] Dassault Systemes, Abaqus, ABAQUS Inc. (2014).
[5] N. Fanaie, S. Aghajani, E. Afsar Dizaj, Strengthening of moment-resisting frame using cable–cylinder bracing, Advances in Structural Engineering 19 (11) (2016) 1736–1754.
[6] G.F. Giaccu, An equivalent frequency approach for determining non-linear effects on pre-tensioned-cable cross-braced structures, Journal of Sound and Vibration 422 (2018) 62–78.
[7] E. Brunesi, D. Bolognini, R. Nascimbene, Evaluation of the shear capacity of precast-prestressed hollow core slabs: numerical and experimental comparisons, Materials and Structures 48 (5) (2015) 1503–1521.
[8] A.I. Al-Negheimish, A.K. El-Sayed, M.O. Khanbari, A.M. Alhozaimy, Long-term deflection of prestressed SCC hollow core slabs, Construction and Building Materials 189 (2018) 181–191.
[9] ACI PRC-209.2-08 Guide for Modeling and Calculating Shrinkage and Creep in Hardened Concrete (2008). ACI Committee 209.
[10] M. Troitsky, Prestressed Steel Bridges: Theory and Design, Van Nostrand Reinhold, New York, 1990.
[11] T.D. Le, T.M. Pham, H. Hao, Y. Hao, Flexural behaviour of precast segmental concrete beams internally prestressed with unbonded CFRP tendons under four-point loading, Engineering Structures 168 (2018) 371–383.
[12] M.A. Pisani, Behaviour under long-term loading of externally prestressed concrete beams, Engineering Structures 160 (2018) 24–33.
[13] T. Lou, S.M. Lopes, A.V. Lopes, Effect of linear transformation on nonlinear behavior of continuous prestressed beams with external FRP cables, Engineering Structures 147 (2017) 410–424.
[14] B.M. Ayyub, Y.G. Sohn, H. Saadatmanesh, Prestressed composite girders under positive moment, Journal of Structural Engineering 116 (11) (1990) 2931–2951.

[15] B.M. Ayyub, Y.G. Sohn, H. Saadatmanesh, Prestressed composite girders. II: Analytical study for negative moment, Journal of Structural Engineering 118 (10) (1992) 2763−2782.
[16] J. Nie, C. Cai, T. Zhou, Y. Li, Experimental and analytical study of prestressed steel−concrete composite beams considering slip effect, Journal of Structural Engineering 133 (4) (2007) 530−540.
[17] H. Zhou, S. Li, L. Chen, C. Zhang, Fire tests on composite steel-concrete beams pre-stressed with external tendons, Journal of Constructional Steel Research 143 (2018) 62−71.
[18] B. Belletti, A. Gasperi, Behavior of prestressed steel beams, Journal of Structural Engineering 136 (9) (2010) 1131−1139.
[19] S. Park, T. Kim, K. Kim, S.-N. Hong, Flexural behavior of steel I-beam prestressed with externally unbonded tendons, Journal of Constructional Steel Research 66 (1) (2010) 125−132.
[20] N. Fanaie, F. Partovi, S. Safaei Faegh, Controlling the deflection of long beams using different patterns of pre-tensioning cables, Scientia Iranica 28 (2) (2021) 598−617.
[21] F. Partovi, N. Fanaie, Controlling deflection of long steel I-shaped girder bridge using two V-shaped pre-tensioning cables, Journal of Central South University 27 (2020) 566−577.
[22] N. Fanaie, F. Partovi, Controlling the deflection of steel cantilever beam using pre-tensioning cable. 3rd International Conference on Steel & Structure, Tehran, Iran (2018).
[23] M.E.M. Kambal, Y. Jia, Theoretical and experimental study on flexural behavior of prestressed steel plate girders, Journal of Constructional Steel Research 142 (2018) 5−16.
[24] W.-F. Zhang, Symmetric and antisymmetric lateral−torsional buckling of prestressed steel I-beams, Thin-Walled Structures 122 (2018) 463−479.
[25] S. Thai, N.-I. Kim, J. Lee, J.-W. Kang, Optimum design of cable nets by using genetic algorithm, International Journal of Steel Structures 17 (3) (2017) 1183−1198.
[26] J.M. Fisher, ANSI/AISC 360-10: Specification for Structural Steel Buildings, American Institute of Steel Construction 13 (2010).
[27] ASTM Standard specification for low-relaxation, seven-wire steel strand for prestressed concrete. ASTM West Conshohocken, PA (2016).